Nondistorting Flattening Maps and the 3-D Visualization of Colon CT Images

Steven Haker, Sigurd Angenent, Allen Tannenbaum*, *Member, IEEE*, and Ron Kikinis

***Abstract*—In this paper, we consider a novel three-dimensional (3-D) visualization technique based on surface flattening for virtual colonoscopy. Such visualization methods could be important in virtual colonoscopy because they have the potential for noninvasively determining the presence of polyps and other pathologies. Further, we demonstrate a method that presents a surface scan of the entire colon as a cine, and affords the viewer the opportunity to examine each point on the surface without distortion.**

We use certain angle-preserving mappings from differential geometry to derive an explicit method for flattening surfaces obtained from 3-D colon computed tomography (CT) imagery. Indeed, we describe a general method based on a discretization of the Laplace–Beltrami operator for flattening a surface into the plane in a conformal manner. From a triangulated surface representation of the colon, we indicate how the procedure may be implemented using a finite element technique, which takes into account special boundary conditions. We also provide simple formulas that may be used in a real-time cine to correct for distortion.

***Index Terms*—Computed tomography (CT) colonography, flattening maps, shape preservation, virtual colonoscopy.**

I. Introduction

THREE-DIMENSIONAL (3-D) visualization is becoming an increasingly important technique in surgical planning, noninvasive diagnosis and treatment, and image-guided surgery. Surface warping and flattening, which allow the easy visualization of highly undulated surfaces, are methods that are becoming increasingly widespread. For example, flattened representations of the brain cortical surface are essential in functional magnetic resonance imaging because we want to show neural activity deep within the folds or sulci of the brain. Three-dimensional visualization is also of great importance in virtual colonoscopy in which we can noninvasively determine the presence of pathologies.

Virtual colonoscopy is currently an active area of research by radiologists as a minimally invasive screening method for the detection of small polyps (see [6] and [7] and the references therein). In the colon, this has become possible because of imaging devices that allow single-breath-hold acquisitions of the entire abdomen at acceptable resolutions. Most reports have focused on methods that use computer graphics to simulate conventional colonoscopic procedures [7], [12], [15]. Other relevant references include McFarland and Valev.

Virtual colonoscopy has some fundamental problems, which it shares with conventional colonoscopy. The most important one is that the navigation using inner views is challenging and it happens frequently that sizable areas are not inspected at all, leading to incomplete examinations. An alternative approach for the inspection of the entire surface of the colon is to simulate the approach favored by pathologists, which involves cutting open the tube represented by the colon, and laying it out flat for a comprehensive inspection. In some very recent work [10], a visualization technique is proposed using cylindrical and planar map projections. It is well known that such projections can cause distortions in shape, as is discussed in [10] and the references therein.

In this paper, we take another approach. We present a method for mapping the colon onto a flat surface in a conformal manner. A *conformal mapping* is a one-to-one mapping between surfaces that preserves angles and, in this sense, preserves the local geometry as well. Our approach to flattening such a surface is based on a certain mathematical technique from Riemann surface theory, which allows us to map any highly undulating tubular surface without handles or self-intersections onto a planar rectangle in a conformal manner. There is some related work in the interesting paper [17] on the topological flattening of a tube onto the plane and its application to virtual colonoscopy. In [17], an electromagnetic field is simulated by placing charges along a fly-through path. The resulting field lines that emanate from a point on the path define a surface whose intersection with the colon surface forms a loop that is flattened into the plane. Our approach differs in that no flight path needs to be calculated and the conformal nature of the flattening allows us to easily correct for distortion.

From a triangulated surface representation of the colon, we indicate how our procedure may be implemented using finite elements. Moreover, we explicitly show how various structures of the colon may be studied using this approach. In contrast to virtual colonoscopy methods that are based on a "fly-through," our method allows the entire colon surface to be viewed at once,

Manuscript received December 15, 1999; revised May 15, 2000. This work was supported in part by the National Science Foundation DMS-9058492, ECS-99700588, NSF-LIS, by the Air Force Office of AF/F49620-98-1-0168, by the Army Research Office DAAG55-98-1-0169, and a MURI Grant. The Associated Editor responsible for coordinating the review of this paper and recommending its publication was N. Ayache. *Asterisk indicates corresponding author*.

S. Haker is with the Department of Diagnostic Radiology and the Department of Computer Science, Yale University, New Haven, CT 06520 USA (e-mail: haker@cs.yale.edu).

S. Angenent is with the Department of Mathematics, University of Wisconsin, Madison, WI 53705 USA.

*A. Tannenbaum is with the Department of Electrical and Computer Engineering and the Department of Biomedical Engineering, Georgia Institute of Technology, Atlanta, GA 30332-0250 USA (e-mail: tannenba@ece.gatech.edu).

R. Kikinis is with the Surgical Planning Lab, Brigham and Women's Hospital, Harvard University, Boston, MA 02115 USA.

Publisher Item Identifier S 0278-0062(00)07331-6.

unobscured by surface folds. Hence, the flattening mapping can be used to obtain an atlas of the given surface in a straightforward, canonical manner. The flattening function is obtained as the solution of a second-order, elliptic partial differential equation (PDE) on the surface to be flattened. From a triangulated representation of the colon surface, we use a finite element procedure to numerically approximate the flattening function. This numerical method involves nearly solving two sparse systems of linear equations and can be accomplished by using standard conjugate gradient techniques.

Once the colon surface has been flattened onto a rectangular region of the plane, we use a method by which the entire colon is presented as a cine, and which allows the viewer to examine each surface point *without distortion* at some time in the image sequence. Thus, in this sense, we achieve 100% view with 0% distortion. In addition to the colon, we have been employing our method in the study of depth maps of bladder images, and in the study of curvatures and polar maps from ultrasound heart images. We are also interested in using our work for the construction of canonical brain models and coordinates on both the gray matter and gray/white matter boundaries from 3-D magnetic resonance data sets [1].

We now summarize the contents of this paper. In Section II, we give a high-level overview of our flattening method. In Section III, we describe the approximation method we employ for numerically computing the flattening mapping based on finite elements. In Section IV, we provide formulas that can be used in real time to create a cine that provides a view of each point of the surface without distortion. Then, in Section V, we illustrate the methodology on some CT colon imagery, and in Section VI, we draw some conclusions about our general approach as well as directions for future research. Finally, in Section VII, we provide some key mathematical details justifying our methodology.

II. General Approach to Colon Flattening

We first consider a mathematical model for the colon surface. Accordingly, let $\Sigma \subset \mathbf{R}^3$ represent an embedded surface (no self-intersections) that is topologically an open-ended cylinder. In the mathematical appendix (see Section VII), we will give more details on the analytical basis for flattening such a surface onto the plane. In this section, we just sketch some of the key points.

We assume that Σ is a smooth manifold. For the finite element method described in the next section, it will be enough to take it as a triangulated surface. We refer the reader to [3] for the basic theory of surfaces of the type we are considering here, and to [11] for the relevant results on partial differential equations.

The boundary of Σ consists of two topological circles, which we will call σ_0 and σ_1. We want to construct a conformal map (i.e., a map that preserves angles and is one-to-one), $f\colon \Sigma \to \mathbf{C}$, which sends Σ to an annulus A such that σ_0 and σ_1 are mapped to the inner and outer boundary circles of A, respectively.

The construction of f begins with finding a solution u to the Dirichlet problem $\Delta u = 0$ on $\Sigma\backslash(\sigma_0 \cup \sigma_1)$, with boundary conditions $u = 0$ on σ_0 and $u = 1$ on σ_1. Here, Δ is the Laplace–Beltrami operator on the surface Σ (see [11]).

We then find a smooth curve C on Σ that runs from σ_0 to σ_1 such that u is strictly increasing along C. This curve defines a cut on Σ, and the cut surface $\Sigma\backslash C$ is conformally equivalent to a rectangle in the plane.

We next compute the harmonic function v, which is conjugate to u by specifying boundary conditions on the cut surface and again solving a Dirichlet problem. The details for this are given in Section VII. The mapping $u+iv\colon \Sigma \to \mathbf{C}$ sends the surface Σ to a rectangle, and its exponential $f = e^{u+iv}$ sends Σ to an annulus.

III. Approximation of the Flattening Function

In the previous section, we outlined the analytical procedure for finding the flattening map f. Here, we will discuss the finite element method for finding an approximation to this mapping. See [8] for details about this method. Because the procedure given here is crucial for the flattening algorithm we have used in our simulations, we will describe this implementation in some detail. In [1], we described a related method for brain flattening. However, because of the differences in topology between the brain and the colon surface, the boundary conditions for the flattening maps are different.

We assume that Σ is a triangulated surface, and we look for a flattening map f which is continuous on Σ and linear on each triangle. Here, we will concentrate on finding u, the method for its conjugate v being similar.

It is a classic result [11] that the harmonic function u is the minimizer of the Dirichlet functional

$$\mathcal{D}(u) := \tfrac{1}{2} \iint_{\Sigma} |\nabla u|^2 \, dS$$
$$u|_{\sigma_0} = 0 \qquad u|_{\sigma_1} = 1$$

where ∇u is the gradient with respect to the induced metric on Σ.

Let $PL(\Sigma)$ denote the finite-dimensional space of piecewise linear functions on Σ. For each vertex $V \in \Sigma$, let ϕ_V be the continuous function such that

$$\begin{aligned} &\phi_V(V) = 1 \\ &\phi_V(W) = 0 \qquad W \neq V \\ &\phi_V \text{ is linear on each triangle.} \end{aligned} \tag{1}$$

Now, this set $\{\phi_V\}$ forms a basis for $PL(\Sigma)$, and so any $u \in PL(\Sigma)$ can be written as

$$u = \sum_{V \in \Sigma} u_V \phi_V.$$

So to approximate the solution to the PDE, we minimize $\mathcal{D}(u)$ over all $u \in PL(\Sigma)$, which satisfy the boundary conditions.

To minimize $\mathcal{D}(u)$, we introduce the matrix

$$D_{VW} = \iint \nabla \phi_V \cdot \nabla \phi_W \, dS$$

for any pair of vertices V, W. It is easy to see that $D_{VW} \neq 0$ if and only if V, W are connected by some edge in the triangulation. We can show (see [8]) that $u = \sum_V u_V \phi_V$ minimizes the

Dirichlet functional over $PL(\Sigma)$ with the boundary conditions, if for each vertex $V \in \Sigma \backslash (\sigma_0 \cup \sigma_1)$

$$\sum_{W \in \Sigma \backslash (\sigma_0 \cup \sigma_1)} D_{VW} u_W = - \sum_{W \in \sigma_1} D_{VW}. \tag{2}$$

A. Computing D_{VW}

Assume $V \in \Sigma \backslash (\sigma_0 \cup \sigma_1)$. If $V \neq W$, the edge VW belongs to two triangles, VWX and VWY. An essential formula from finite element theory [8], then says that

$$D_{VW} = -\tfrac{1}{2}\{\cot \angle X + \cot \angle Y\}$$

where $\angle X$ is the angle at the vertex X in the triangle VWX, and $\angle Y$ is the angle at the vertex Y in the triangle VWY.

If $V = W$, we have

$$D_{VV} = - \sum_{W \neq V} D_{VW}.$$

B. Summary of Method

We may summarize the finite element procedure for the construction of the flattening map as follows:

1) Compute the D_{VW}.
2) Solve the linear equation (2) to obtain the piecewise linear harmonic function $u = \sum_V u_V \phi_V$.
3) Cut the surface from σ_0 to σ_1, and compute the boundary values of v by integrating $\partial u / \partial n$ (the derivative of u in the normal direction [11]) around the boundary. Use finite elements to solve for v. To find a cut, we may start at a vertex on σ_0, and move from each vertex to the adjacent vertex that has the largest value of u associated with it. The maximum principle implies that there is always an adjacent vertex with a larger value of u than the current vertex. Also, in this way, we make a cut that follows closely the gradient of u while remaining on edges of triangles. Thus, our flattened image will be roughly rectangular in shape.

IV. Inspection and Distortion Removal

In practice, once the colon surface has been flattened into a rectangular shape, it will need to be visually inspected for various structures. In this section, we present a simple technique by which the entire colon surface can be presented to the viewer as a sequence of images or cine. In addition, this scanning method allows the viewer to examine each surface point without distortion at some time in the cine. Here, we will say a mapping is without distortion at a point if it preserves the intrinsic distance there.

It is well known that a surface cannot in general be flattened onto the plane without some distortion somewhere (see [4]). For conformal flattenings, we may show that the Gaussian curvature K and conformal distortion factor $\phi > 0$ are related by the nonlinear PDE (see [4])

$$K = \frac{-1}{\phi^2} \Delta \log \phi. \tag{3}$$

This roughly shows that the greater the Gaussian curvature, the larger the conformal distortion. The relationship is complicated, however, because distortion and curvature are related via a nonlinear partial differential equation.

On the other hand, it is possible to achieve a surface flattening that is free of distortion *along some curve*. A simple example of this is the familiar Mercator projection of the earth, in which the equator appears without distortion. In our case, the distortion-free curve will be a level set of the harmonic function u described above (essentially a loop around the tubular colon surface), and it will correspond to the vertical line through the center of a frame in the cine. This line is orthogonal to the direction of the scan, so that every point of the colon surface is exhibited at some time without distortion.

Explicitly, suppose we have conformally flattened the colon surface onto a rectangle $R = [0, u_{\max}] \times [-\pi, \pi]$. Let F be the inverse of this mapping, and let $\phi^2 = \phi^2(u, v)$ be the amount by which F scales a small area near (u, v); i.e., let $\phi > 0$ be the "conformal factor" for F. Fix $w > 0$, and for each $u_0 \in [0, u_{\max}]$, define a subset $R_0 = ([u_0 - w, u_0 + w] \times [-\pi, \pi]) \cap R$ that will correspond to the contents of a cine frame. We define a mapping

$$(\hat{u}, \hat{v}) = G(u, v) = \left(\int_{u_0}^{u} \phi(\mu, v)\, d\mu, \int_0^v \phi(u_0, \nu)\, d\nu \right)$$

from R_0 to $\mathbf{C}$ that has differential

$$dG(u, v) = \begin{pmatrix} \hat{u}_u & \hat{u}_v \\ \hat{v}_u & \hat{v}_v \end{pmatrix} = \begin{pmatrix} \phi(u, v) & \displaystyle\int_{u_0}^{u} \phi_v(\mu, v)\, d\mu \\ 0 & \phi(u_0, v) \end{pmatrix}$$

and in particular $dG(u_0, v) = \phi(u_0, v) \times \left(\begin{smallmatrix} 1 & 0 \\ 0 & 1 \end{smallmatrix}\right)$. The conformality of the flattening map, together with this value for $dG(u_0, v)$, implies that the composition of the flattening map with G sends the level set loop $\{u = u_0\}$ on the colon surface to the vertical line $\{\hat{u} = 0\}$ in the $\hat{u}$–$\hat{v}$-plane without distortion. In addition, it follows from the formula for dG that lengths measured in the $\hat{u}$-direction accurately reflect the lengths of corresponding curves on the colon surface.

V. Computer Simulations

We tested our algorithm on three different data sets provided to us by the Surgical Planning Laboratory of Brigham and Women's Hospital. Because the results were similar in each case, we just include here one of the sets. This example consists in a test of flattening the colon surface contained in a $256 \times 256 \times 124$ CT colon image. Four slices from this data set are shown in Fig. 1.

First, using the fast segmentation methods of [9] and [14], we found the colon surface. Unfortunately, the segmentation algorithm does not guarantee that the surface found will be a topological cylinder. In fact, it may contain numerous minute handles that develop because the boundary of the colon, as represented in the data set, may not be sharp. We used a morphological-based method [5] by which these handles can be effectively removed and a surface that has the topology of a closed-ended cylinder can be extracted. This is done in such a way that the large-scale geometry of the surface is not adversely affected.

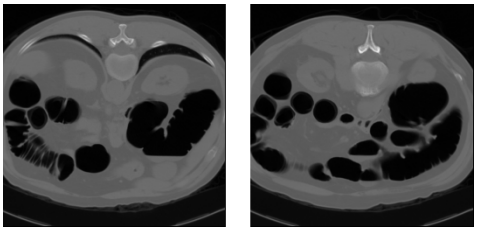

Fig. 1. Two slices of colon CT data.

We then created a triangularization of this surface using the Visualization Toolkit [13]. (The newest version of VTK is available at the website www.kitware.com.) Next, the triangularized surface was smoothed slightly to reduce the effects of aliasing. This was done by using a flow based on mean curvature. The triangles making up the two ends of the tubular surface were then removed to produce an open-ended tube with two boundary curves.

Next, as described in the Section III, we found the harmonic function u, made a cut along the colon surface from one bounding curve to the other, and then found the conjugate harmonic function v to complete the calculation of the flattening map onto a nearly rectangular region of the plane. We tried cuts starting from several different boundary points and found no significant changes from the results reported here; this independence of path is in agreement with the mathematical theory.

For purposes of visualization, we colored points of the colon surface according to mean curvature, and then applied these same colors to the flattened image in the plane. This gave an elegant way to visualize the structure of the colon that is a twisted, undulating tube. Our segmentation method is a so-called "level-set" method, in which the colon surface to extract is defined implicitly as the zero level set $\{(x, y, z)|\Psi(x, y, z) \equiv 0\}$ of a function Ψ defined on the 3-D volume. It is well known that the Gaussian and mean curvatures of such an isosurface can be calculated from the derivatives of Ψ; doing so allows us to avoid having to make these calculations on the triangulated surface after extraction. In fact, we may use the function Ψ to determine the entire second fundamental form for the isosurface, using the formula

$$II = \frac{-1}{||\nabla\Psi||} T^t H_\Psi T$$

where H_Ψ is the 3×3 Hessian matrix of second derivatives of Ψ, and T is a 3×2 matrix whose columns are arbitrary orthonormal vectors perpendicular to the surface normal $N = \nabla\Psi/||\nabla\Psi||$. The eigenvectors e_1 and e_2 of II yield the principal directions (the directions in which the degree of surface bending is extremal) as Te_1 and Te_2, whereas the eigenvalues k_1, k_2 are the corresponding principal curvatures. The Gaussian curvature can then be found by $K = k_1 k_2 = \det(II)$, and the mean curvature by $H = (1/2)(k_1 + k_2) = (1/2)\text{trace}(II)$.

In Fig. 2, we show three different views of the segmented colon surface and its flattened representation colored according to mean curvature. A small circled region visible at the bottom of the flattened surface, and the corresponding region of the original surface, is shown in detail in Fig. 3. In Fig. 4, we show an interior "fly-through" view of the colon image, and its flattened representation. Notice how much easier it is to get a view of the whole interior region in this manner.

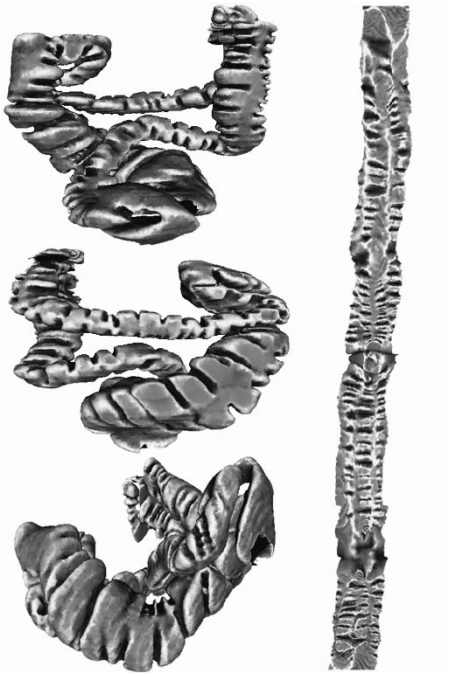

Fig. 2. Segmented colon and flattened representation.

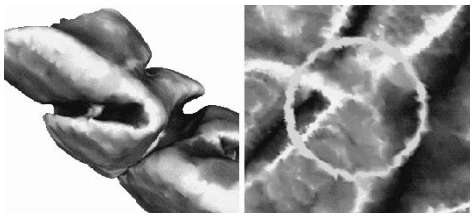

Fig. 3. Region of interest and flattened representation.

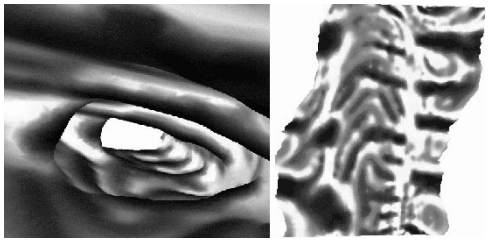

Fig. 4. "Fly-through" view and flattened representation.

We would expect polyps to have relatively high Gaussian curvature compared with the flatter surrounding colon surface. Further, these areas should be convex with respect to the colon interior, and thus have positive mean curvature with respect to the outward surface normal. This suggests that as an alternative scheme for visualization, we color the flattened surface according to the Gaussian curvature of the colon surface, but only where both the Gaussian and mean curvatures of the colon surface are positive. The other areas may be colored with some neutral color. This alone, however, is not satisfactory for visualization of the flattened colon because the folds of the colon will not be represented. One solution to this problem is to use

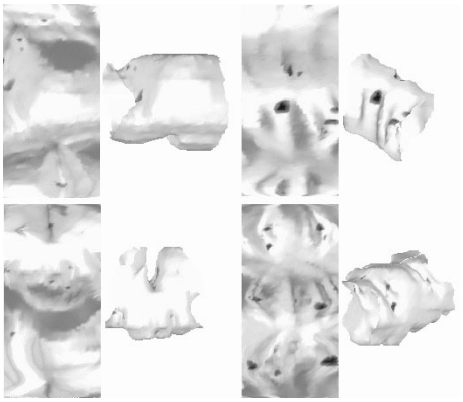

Fig. 5. Frames from distortion-correcting cine with original surface.

shading maps, an idea from computer graphics. The idea is to translate surface normals from the original surface to the corresponding point on the flattened surface. When rendered under identical lighting conditions, the original surface and the flattened surface with these "pseudonormals" will have similar appearances, because of similar shading. This allows us to color the surface any way we wish and still have the surface folds distinguishable in the flattened representation.

We used this shading map in conjunction with the formulas in Section IV to create a distortion correcting cine of a scan of the colon surface. To make numeric integration fast and simple, we interpolated the function ϕ (defined on the rectangular representation of the colon in the u–v-plane) onto an equally spaced grid. For each particular value u_0 of u, increasing from 0 to $u_{\max}$ on this grid, we mapped the corresponding subrectangle R_0 to the $\hat{u}$–$\hat{v}$-plane, as described in Section IV. We found that this could be done in real time. Four frames from the resulting cine can be seen in Fig. 5. For comparison, we show an exterior view of the portion of the original colon surface corresponding to each frame. As the cine progresses, the vertical line through the center of the frame is a distortion-correcting representation of a loop on the colon surface. These loops sweep continuously over the colon surface from end to end, and thus every surface point is presented to the viewer in some frame without distortion. Further, the mapping to the $\hat{u}$–$\hat{v}$-plane is a continuous function of time, and so there is no jumping between frames. The fact that distances in the $\hat{u}$-direction are the same as corresponding distances on the surface seems to help in keeping distortion to an acceptable level even off the vertical center line. Notice that the coloring and shading scheme indicate the convex areas and surface folds. One can see the cine on our web site http://noodle.med.yale.edu/~haker/colonoscopy. We are currently investigating the usefulness of this visualization scheme for the detection of polyps in a clinical setting.

VI. Conclusion

In this note, we described a procedure based on conformal geometry and harmonic analysis for the construction of a flattening map of a colon surface derived from volumetric CT data. Further, we presented a numerical algorithm that finds this map by a finite element technique. Finally, we demonstrated formulas that can be used in a cine to provide a distortion-free view of every point on the colon surface. Additional details on the underlying mathematics, numerics and an application to 3-D brain imagery may be found in [1].

Deformations of highly undulated surfaces have applications in the analysis of military as well as medical imagery. They also have applications in computer graphics, for example, in the area of texture mapping. We believe that the angle-preserving mapping methods described here will prove to be useful in these areas.

We have also been considering area-preserving flattening maps of minimal distortion as a way to optimize the tradeoff between exact area-preservation and minimal angle deviation. It is mathematically impossible to have both the area and angles preserved everywhere in a diffeomorphism between surfaces unless the two surfaces have the same Gaussian curvature; see [4] for all of the relevant results and definitions. Thus, this type of tradeoff is probably the best that we can do. For the mathematical details, see [2]. We will be applying this methodology to both brain and colon imagery in our future work.

VII. Mathematical Appendix

We use the notation of Section II. We will fill in the details of the high-level algorithm for the construction the flattening map $f\colon \Sigma \to \mathbf{C}$.

1) Let u be the solution of the Dirichlet problem

$$\begin{aligned} \Delta u &= 0 \text{ on } \Sigma \backslash (\sigma_0 \cup \sigma_1), \\ u &= 0 \text{ on } \sigma_0, \\ u &= 1 \text{ on } \sigma_1. \end{aligned} \tag{4}$$

Here, Δ represents the Laplace–Beltrami operator on the surface Σ. This second-order partial differential operator is intrinsic to the surface and is a generalization of the standard Laplacian in the plane. From the standard theory of partial differential equations [11], u exists and is unique.

2) Let C be a smooth curve on Σ that runs from σ_0 to σ_1 such that u is strictly increasing along C. The maximum principle implies the existence of such a curve. This curve defines a cut on Σ, and the cut surface $\Sigma \backslash C$ is conformally equivalent to a rectangle in the plane.

Let B be the oriented boundary of this cut surface; i.e., let B run around σ_0, then along C to σ_1, around σ_1, then along C again in the opposite direction to σ_0. The closed path B must run around σ_0 and σ_1 in a fashion consistent with an orientation given on the surface Σ.

We want to compute the harmonic function v that is conjugate to u by specifying boundary conditions on the cut surface and again solving a Dirichlet problem. Let $\partial/\partial s$ and $\partial/\partial n$ denote tangential and normal derivatives, respectively. By the Cauchy–Riemann equations, we have

$$\frac{\partial v}{\partial s} = \frac{\partial u}{\partial n}$$

on B and so the boundary values of v may be found by integration along B

$$v(\zeta) = \int_{\zeta_0}^{\zeta} \frac{\partial v}{\partial s}\, ds = \int_{\zeta_0}^{\zeta} \frac{\partial u}{\partial n}\, ds$$

where here s is the arc-length along B. Because u is harmonic, the divergence theorem guarantees that $\oint_B (\partial u/\partial n)\, ds = 0$, and so v is smooth (periodic) on B.

Note that if we choose C so that it follows the gradient of u from σ_0 to σ_1, we would have $\partial u/\partial n = 0$ along C, and so v would be constant on B along the parts corresponding to C.

3) The component v of the rectangular map $f_1 = u + iv$ is then found by solving the Dirichlet problem using the calculated boundary values for v. If C is chosen to follow along the gradient of u, the image of Σ in the u–v-plane under f_1 will be a rectangle of width 1 and some height h. For other curves C, along which u is monotone, the image will be a region in the u–v-plane among the lines $u = 0$, $u = 1$, the graph of a function $g = g(u)$, and a copy of the graph of g shifted vertically by a constant, i.e., $g(u) + h$. The fact that the distance across the region vertically is constant is again a consequence of the divergence theorem. We may now dilate the flattened rectangular image of Σ under f_1 homothetically, and so we may assume that $h = 2\pi$. We may then map the surface to a true cylinder of radius 1 by simply "rolling up" the flattened image. We may also map it to an annulus via $f = e^{f_1}$, effectively reconnecting the image of the surface smoothly across the cut. We may then map it to the sphere using stereographic projection, if desired. In practice, we have found rectangular mapping to be the most natural representation of the flattened colon. The existence of the cut in the rectangular mapping does not present a problem for visualization; the constant height of the rectangular image allows us to extend it periodically above and below the cut.

Remark: The annular map f is unique up to a dilation, rotation, and translation. That is, any other conformal $\hat{f}$: $\Sigma \to \mathbf{C}$ that maps Σ to an annulus and σ_1 to its outer boundary is given by

$$\hat{f} = \alpha f + \beta \tag{5}$$

for some constants α, $\beta \in \mathbf{C}$.

REFERENCES

[1] S. Angenent, S. Haker, A. Tannenbaum, and R. Kikinis, "Laplace–Beltrami operator and brain surface flattening," *IEEE Trans. Med. Imag.*, vol. 18, pp. 700–711, 1999.

[2] ——, "On area preserving mappings of minimal distortion," in *System Theory: Modeling, Analysis, and Control*, T. Djaferis and I. Schick, Eds. Holland: Kluwer, 1999, pp. 275–287.

[3] H. Farkas and I. Kra, *Riemann Surfaces*. New York: Springer-Verlag, 1991.

[4] M. P. Do Carmo, *Riemannian Geometry*. Englewood Cliffs, NJ: Prentice-Hall, 1992.

[5] S. Haker, "Extracting simply connected iso-surfaces from volumetric data,", submitted for publication.

[6] A. Hara, C. Johnson, and J. Reed, "Detection of colorectal polyps by computed tomographic colography: Feasibility of a novel technique," *Gastroenterology*, vol. 110, pp. 284–290, 1996.

[7] A. Hara, C. Johnson, J. Reed, R. Ehman, and D. Ilstrup, "Colorectal polyp detection with CT colography: Two- versus three-dimensional techniques," *Radiology*, vol. 200, pp. 49–54, 1996.

[8] T. Hughes, *The Finite Element Method*. Englewood Cliffs, NJ: Prentice-Hall, 1987.

[9] S. Kichenasamy, P. Olver, A. Tannenbaum, and A. Yezzi, "Conformal curvature flows: From phase transitions to active contours," *Arch. Rat. Mech. Anal.*, vol. 134, pp. 275–301, 1996.

[10] D. Paik, C. Beaulieu, R. Jeffrey, C. Karadi, and S. Napel, "Visualization modes for CT colonography using cylindrical and planar map projections," Dept. Radiol., Stanford Univ. School of Med., Stanford, CA, Tech. Rep., 1999.

[11] J. Rauch, *Partial Differential Equations*. New York: Springer-Verlag, 1991.

[12] G. Rubin, S. Napel, and A. Leung, "Volumetric analysis of volumetric data: Achieving a paradigm shift," *Radiology*, vol. 200, pp. 312–317, 1996.

[13] W. Schroeder, H. Martin, and B. Lorensen, *The Visualization Toolkit*. Englewood Cliffs, NJ: Prentice-Hall, 1996.

[14] K. Siddiqi, A. Tannenbaum, and S. Zucker, "Area and length minimizing flows for image segmentation," *IEEE Trans. Image Processing*, vol. 7, pp. 433–444, 1998.

[15] D. Vining, "Virtual endoscopy: Is it reality," *Radiology*, vol. 200, pp. 30–31, 1996.

[16] B. Wandell, S. Engel, and H. Hel-Or, "Creating images of the flattened cortical sheet," *Invest. Opth. Vis. Sci.*, vol. 36, 1996.

[17] G. Wang, E. McFarland, B. Brown, and M. Vannier, "GI tract unraveling with curved cross sections," *IEEE Trans. Med. Imag.*, vol. 17, pp. 318–322, 1998.